Supporting Information

Probing the robustness of inhibitors of tuberculosis aminoglycoside resistance enzyme Eis by mutagenesis

Keith D. Green,[a,†] Ankita Punetha,[a,†] Caixia Hou,[a] Sylvie Garneau-Tsodikova,[a,*] Oleg V. Tsodikov[a,*]

[a] University of Kentucky, College of Pharmacy, Department of Pharmaceutical Sciences, Lexington, KY, USA, 40536-0596.

† These authors contributed equally to this work.

* Correspondence to: sylviegtsodikova@uky.edu or oleg.tsodikov@uky.edu

12 pages

3 figures

3 tables

Cloning of Eis mutants. Primers used in the amplification of the mutant *eis* genes are listed in Table S1. PCRs were performed using the *eis* gene in pET28a (*eis*-pET28a) as a template. Single-point mutants were constructed using the single overlap extension (SOE) method, which consisted of two rounds of PCRs.[1] The first round consisted of two PCRs, one using the *eis wt* 5'-primer with the *eis* mutant 3'-primer, and the other using the *eis wt* 3'-primer with the *eis* mutant 5'-primer. The second round of PCRs used the two products created in the first round in one mixture with the *eis wt* 5'- and 3'-primers to generate the desired *eis* mutant genes. After the PCRs were complete and the *eis* mutant genes isolated, the PCR products were digested with *Nde*I and *Bam*HI and ligated into linerarized pET28a vector with the corresponding sticky ends, yielding the point mutants D26A, W36A, W36R, R37A, R37G, L63A, M65A, and S83G. The expression constructs for F24A and F84A mutants were generated previously.[1] The plasmids were transformed into chemically competent *E. coli* TOP10 cells. Mutations were confirmed by DNA sequencing performed at Eurofins (Louisville, KY).

Table S1. Primers used for the PCR amplification of the *eis* gene from *M. tuberculosis* and for the constructions of its mutants.

Gene	5'-primer	3'-primer
eis_wt	CCGCGGCATATGCTACAGTCGGATTC	CTAGCAGGATCCTCAGAACTCGAACGCG
eis_D26A	GCCAGTTTCACCgcgTTCATCGGCCCT	AGGGCCGATGAAcgcGGTGAAACTGGC
eis_W36A	TCAGCGACCGCCgcgCGGACCCTGGTG	CACCAGGGTCCGcgcGGCGGTCGCTGA
eis_W36R	TCAGCGACCGCCcgcCGGACCCTGGTG	CACCAGGGTCCGgcgGGCGGTCGCTGA
eis_R37A	GCGACCGCCTGGgcgACCCTGGTGCC	GGGCACCAGGGTcgcCCAGGCGGTCGC
eis_R37G	GCGACCGCCTGGggcACCCTGGTGCCC	GGGCACCAGGGTgccCCAGGCGGTCGC
eis_L63A	GTCGGGATGGCGgcgTACATGGATCTG	CAGATCCATGTAcgcCCGCCATCCCGAC
eis_M65A	ATGGCGCTGTACgcgGATCTGCGGTTG	CAACCGCAGATCcgcGTACAGCGCCAT
eis_S83G	ACCGCCGGTCTCggcTTCGTCGCGGTG	CACCGCGACGAAgccGAGACCGGCGGT

The introduced cut sites are underlined for each primer. The 5'-primer introduced a *Nde*I restriction site and the 3'-primer introduced a *Bam*HI restriction site. The mutation sites are indicated in lower case.

Overexpression and purification of Eis and its mutants. The plasmids containing the *eis wt* and *eis* mutants genes were transformed into *E. coli* BL21 (DE3), and expressed and purified as previously reported.[1] Briefly, Luria-Bertani (LB) broth was inoculated with a dense culture of bacteria containing the gene of interest (3 mL culture into 1 L LB broth). Cultures were grown at 37 °C with shaking (200 rpm) until an attenuance of 0.4 (at 600 nm) was obtained, at which time the temperature was lowered to 20 °C. Once the cultures reached an attenuance of 0.6 (at 600 nm), protein expression was induced with 0.5 mM IPTG (final concentration). Protein production was continued overnight (~18 h) at 20 °C. The cells were harvested by centrifugation (5,500×g, 4 °C, 10 min). The cell pellets were resuspended in Buffer A (300 mM NaCl, 50 mM sodium phosphate buffer pH 8.0, and 10% *v*/*v* glycerol) and lysed by four rounds of sonication (2 s “on”, 10 s “off”,

for two min). Cell lysates were clarified by centrifugation (40,000×g, 45 min, 4 °C) and the supernatants were incubated with a Ni^{II}-NTA affinity resin for 2 h with gentle rocking. Increasing concentrations of imidazole (10 mL of 5 mM, 2×5 mL of 20 mM, 2×5 mL of 40 mM, and 3×5 mL of 250 mM) in Buffer A were used to elute the proteins of interest as monitored by SDS-PAGE. Fractions containing Eis proteins were pooled and dialyzed in 50 mM Tris pH 8.0 with 10% *v*/*v* glycerol prior to concentration. The protein was concentrated with an Amicon Ultra (10,000 MWCO) centrifugal filter device (Millipore). Protein yields (in mg/L culture) were 2.0 (Eis_wt), 1.1 (Eis_D26A), 2.1 (Eis_W36A), 2.2 (Eis_W36R), 1.8 (Eis_R37A), 0.9 (Eis_R37G), 1.7 (Eis_L63A), 1.8 (Eis_M65A), 3.2 (Eis_S83G), and 0.8 (Eis_F84A). All proteins were stored at 4 °C and experiments were performed within a week to ensure optimum protein activity.

Protein expression and purification for X-ray crystallographic studies. Analogously to our previous structural studies of Eis-aminoglycoside and Eis-inhibitor complexes,[2-6] for the crystallographic studies reported here we used the Eis construct described above, but bearing a C204A mutation. This mutation does not perturb Eis activity or assembly, and it prevents CoA used in crystallization drops from crosslinking to Cys204 upon oxidation and obstructing the access to the active site of the enzyme. Cys204 lies outside of the active site, but it is close enough for the crosslinked CoA to reach the substrate binding pocket. For expression and purification of Eis_C204A we followed the protocol described in the previous section, but instead of dialysis, the protein eluted from the Ni^{II}-chelating column with the elution buffer containing 250 mM imidazole was passed through a size-exclusion HiPrep 26/60 Sephacryl HR S-200 column (GE Healthcare) equilibrated in gel filtration buffer (40 mM Tris-HCl pH 8.0, 100 mM NaCl, and 2 mM β-mercaptoethanol). The fractions containing Eis were pooled and concentrated in an Amicon Ultra (10,000 MWCO) centrifugal filter device (Millipore) to 9 mg/mL. The concentrated Eis protein was stored on ice at 4 °C during crystallization experiments.

Determination of kinetic parameters for wt and mutant Eis in the absence and in the presence of inhibitors. The steady-state kinetic parameters (K_m and k_{cat}) for KAN acetylation by wt and mutant Eis enzymes were determined by using a previously described UV-Vis assay.[7] Briefly, reactions were initiated by adding a 50 μL solution containing DTNB (8 mM) and various concentrations of KAN (0-1 mM for all enzymes except for Eis_R37 mutants where the upper

limit was 5 mM) either without inhibitors or with an inhibitor at the specified concentration to 150 μL mixture of Eis enzyme (0.33 μM) and AcCoA (667 μM) in Tris-HCl (50 mM, pH 8.0). Inhibitors **1**, **2** and **3** (SGT449, SGT335, and SGT416) were synthesized as described previously and dissolved in DMSO at 10 mM.[2-3, 6] Prior to mixing with KAN, the inhibitors were diluted to a 40-fold higher concentration that that used in a given reaction with DMSO. The assays were performed in triplicate. The reactions were monitored for 15 min, taking measurements every 30 s at 25 °C on a SpectraMax M5 plate reader. The first 5-10 min of the reactions were used to calculate the initial rates of the reactions plotted in Fig. S1. Nonlinear regression fitting procedure using the Michaelis-Menten equation in SigmaPlot 13.0 (Systat) yielded best-fit curves shown in Fig. S1 and the values listed in Tables 2 and S2.

Table S2. Kinetic parameters from each triplicate experiment for Eis enzymes with various concentrations of inhibitors.

Enzyme	Cpd	Concentration (μM)	K_m (μM)	k_{cat} (min^{-1})	k_{cat}/K_m ($min^{-1}\mu M^{-1}$)
Eis_wt	**1** (SGT449)	0	428 ± 67	12.2 ± 0.8	0.028 ± 0.004
		0.1	597 ± 144	7.85 ± 0.92	0.013 ± 0.004
		0.2	1080 ± 420	7.06 ± 1.67	0.007 ± 0.003
		0.3	839 ± 575	5.69 ± 2.17	0.007 ± 0.005
	2 (SGT335)	0	407 ± 33	12.6 ± 0.4	0.031 ± 0.003
		0.125	676 ± 36	11.3 ± 0.3	0.017 ± 0001
		0.25	436 ± 64	6.19 ± 0.39	0.014 ± 0.002
		0.5	1250 ± 480	6.66 ± 1.62	0.005 ± 0.002
	3 (SGT416)	0	819 ± 169	18.2 ± 2.0	0.022 ± 0.005
		0.05	1530 ± 600	17.1 ± 4.6	0.011 ± 0.005
		0.10	1070 ± 400	16.1 ± 3.7	0.015 ± 0.007
		0.15	5740 ± 3640	39.1 ± 21.7	0.007 ± 0.005
Eis_D26A	--	--	1280 ± 360	14.1 ± 2.5	0.011 ± 0.004
Eis_W36A	--	--	556 ± 148	8.30 ± 1.04	0.015 ± 0.004
Eis_W36R	**1** (SGT449)	0	352 ± 77	4.37 ± 0.38	0.012 ± 0.003
		0.02	299 ± 56	3.27 ± 0.23	0.011 ± 0.002
		0.04	246 ± 54	2.88 ± 0.22	0.012 ± 0.003
		0.1	275 ± 44	2.05 ± 0.12	0.007 ± 0.001
Eis_R37A	--	--	1010 ± 220	1.93 ± 0.14	0.008 ± 0.002
	1 (SGT449)	0	652 ± 134	10.1 ± 0.7	0.015 ± 0.003
		0.2	773 ± 94	4.79 ± 0.21	0.006 ± 0.001
		0.4	989 ± 244	6.20 ± 0.58	0.006 ± 0.002
		0.8	1130 ± 248	4.47 ± 0.39	0.004 ± 0.001
	2 (SGT335)	0	1050 ± 175	9.51 ± 0.62	0.009 ± 0.002
		0.125	1060 ± 115	7.87 ± 0.33	0.007 ± 0.001
		0.25	2240 ± 390	8.43 ± 0.71	0.004 ± 0.001
		0.5	1940 ± 224	7.01 ± 0.39	0.004 ± 0.0005
	3 (SGT416)	0	1210 ± 110	8.98 ± 0.33	0.007 ± 0.001
		0.15	1390 ± 124	7.81 ± 0.29	0.006 ± 0.001
		0.25	1620 ± 185	8.07 ± 0.40	0.005 ± 0.001
		0.6	3710 ± 786	8.17 ± 0.96	0.002 ± 0.0005
Eis_R37G	**2** (SGT335)	0	642 ± 122	12.8 ± 0.8	0.020 ± 0.004
		0.5	695 ± 120	10.8 ± 0.6	0.016 ± 0.003
		1.0	807 ± 121	7.68 ± 0.42	0.010 ± 0.002
		2.0	795 ± 75	5.14 ± 0.18	0.006 ± 0.001
	3 (SGT416)	0	750 ± 163	13.0 ± 1.0	0.017 ± 0.004
		0.8	1060 ± 170	8.85 ± 0.54	0.008 ± 0.001
		1.7	939 ± 158	6.94 ± 0.44	0.007 ± 0.001
		2.5	1080 ± 220	5.16 ± 0.40	0.005 ± 0.001
Eis_L63A	**2** (SGT335)	0	577 ± 47	20.9 ± 0.9	0.036 ± 0.003
		0.125	414 ± 42	14.0 ± 0.6	0.034 ± 0.004
		0.25	401 ± 83	8.98 ± 0.82	0.022 ± 0.005
		0.5	466 ± 89	7.77 ± 0.68	0.017 ± 0.003
	3 (SGT416)	0	391 ± 47	17.9 ± 0.9	0.046 ± 0.006
		0.05	829 ± 124	15.2 ± 1.3	0.018 ± 0.003
		0.15	527 ± 113	9.38 ± 0.97	0.018 ± 0.004
		0.25	592 ± 110	9.02 ± 0.8	0.015 ± 0.003
Eis_M65A	**1** (SGT449)	0	247 ± 19	29.7 ± 0.9	0.122 ± 0.015
		0.32	238 ± 8	19.6 ± 0.3	0.083 ± 0.003
		0.64	332 ± 41	17.9 ± 0.9	0.054 ± 0.007
		0.75	312 ± 49	18.4 ± 1.2	0.059 ± 0.010
Eis_S83G	**1** (SGT449)	0	384 ± 90	21.1 ± 2.0	0.055 ± 0.013
		0.64	392 ± 68	16.8 ± 1.2	0.043 ± 0.008
		0.8	351 ± 51	15.5 ± 0.9	0.044 ± 0.007
		2	503 ± 133	14.2 ± 1.7	0.028 ± 0.008
	3 (SGT416)	0	480 ± 57	22.7 ± 1.2	0.047 ± 0.006
		0.04	808 ± 130	17.4 ± 1.5	0.022 ± 0.004
		0.12	825 ± 135	14.7 ± 1.3	0.018 ± 0.003
		0.2	585 ± 188	12.3 ± 1.9	0.021 ± 0.008
Eis_F84A	--	--	569 ± 94	8.52 ± 0.67	0.015 ± 0.003

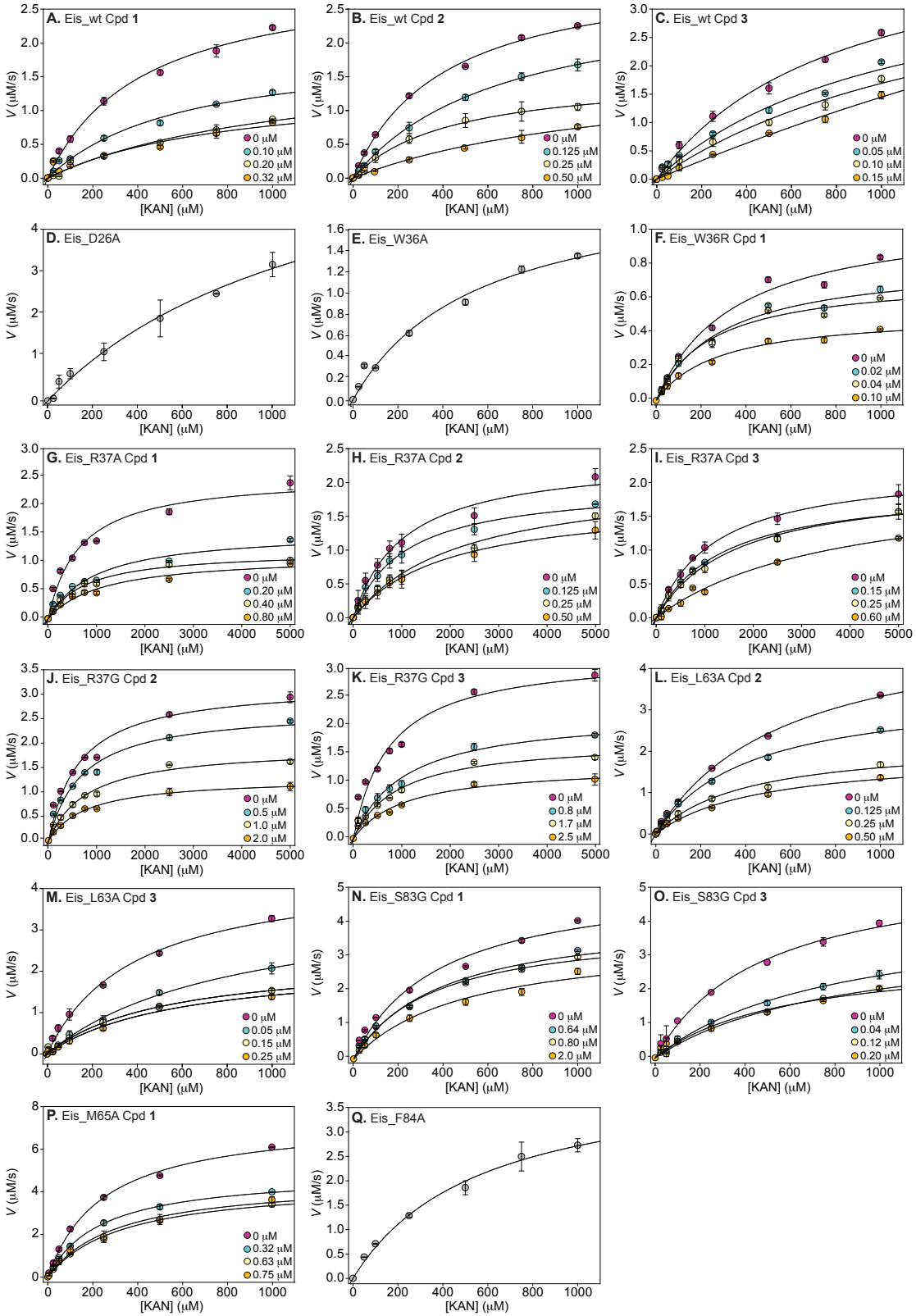

Fig. S1: Michaelis-Menten curves for kinetic data of all Eis enzymes (pink or gray circles). The data for inhibitor concentrations below, near, and above IC_{50} are shown by blue, yellow, and orange circles, respectively.

Determination of inhibitor potency. IC_{50} values were determined using the same assay as that used to determine the kinetic parameters. Compounds **1-3** (5 μL of 10 mM in DMSO) were diluted to 400 μM in Tris-HCl (120 μL, 50 mM, pH 8.0) followed by serial 5-fold dilutions in 50 mM Tris-HCl, pH 8.0 in a 96-well plate, where 25 μL of the previous solution is added to 100 μL etc, so that each well contained 100 μL of the inhibitor at different concentrations. A mixture (50 μL) of Eis (1 μM), KAN (400 μM), and Tris-HCl (50 mM, pH 8.0) was added to the inhibitor solutions and incubated for 5 min. Reactions were initiated by the addition (50 μL) of AcCoA (2 mM), DTNB (8 mM), and Tris-HCl (50 mM, pH 8.0). Initial rates (first 2-5 min of reaction) were calculated and used to determine the IC_{50} values. All assays were performed at least in triplicate. Data were fit to a Hill-plot fit using KaleidaGraph 4.1 software to determine the IC_{50} values. All IC_{50} values are listed in Table 3 and examples of IC_{50} curves are presented in Fig. S2.

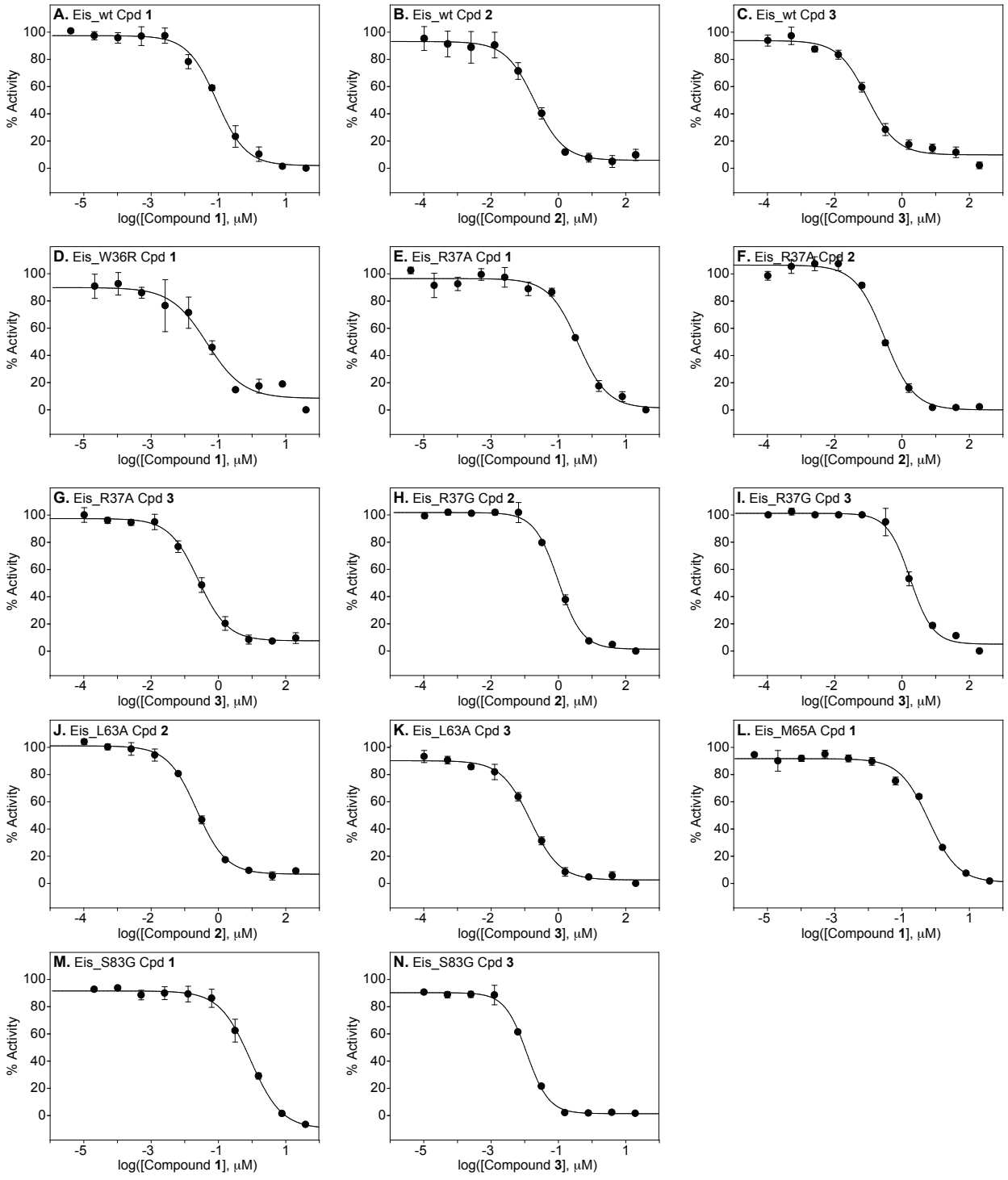

Fig. S2: IC_{50} curves for all combinations of Eis enzymes and compounds that showed inhibition.

Determination of mode of inhibition for compounds 1-3. The inhibition kinetics were determined as described in the "Determination of kinetic parameters" section. The V_{max} and K_m values obtained as described in that section were used, without any conversion, in nonlinear

regression fitting to the competitive inhibition rate law (Eq. 1) with SigmaPlot to obtain the K_i values, which are presented in Table 3. The same data were plotted in a double reciprocal Lineweaver-Burk plots to visualize the competitive mode of inhibition. Representative plots are presented in Fig. S3.

Equation 1: $$v = \frac{V_{max}[S]}{[S]+K_m\left(1+\frac{[I]}{K_i}\right)}$$

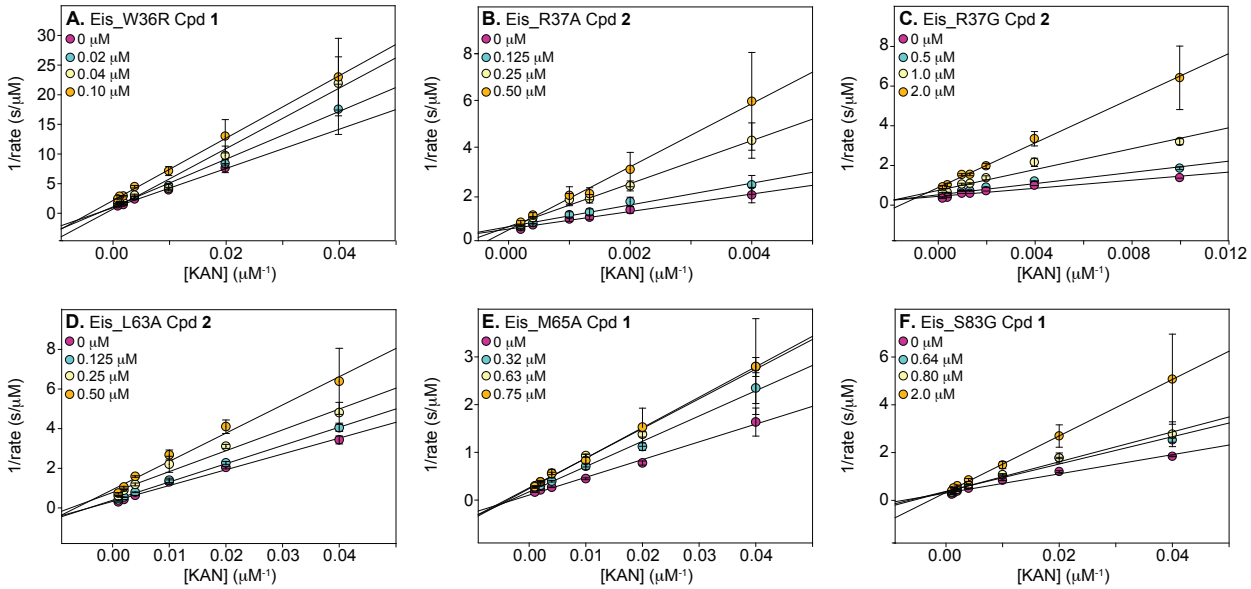

Fig. S3: Lineweaver-Burk plots of selected combinations of Eis enzyme and compounds showing that the compounds still interact with the enzyme in a mixed-competitive manner.

Crystallization of Eis-inhibitor complexes and crystal structure determination. The crystals of Eis-inhibitor complexes were grown by vapor diffusion in hanging drops at 22 °C. The 2 μL drops contained 1 μL of EisC204A (9.27 mg/mL), KAN (10 mM) and CoA (8 mM) mixed with 1 μL of the reservoir solution (100 mM Tris-HCl, pH 8.0, 10% *w*/*v* PEG 8000, and 400 mM $(NH_4)_2SO_4$). The drops were equilibrated against 1 mL of the reservoir solution and crystals were obtained within 1-2 weeks. The $(NH_4)_2SO_4$, CoA, and KAN were then removed by gradual transfer of crystals into the reservoir solution lacking these components (100 mM Tris-HCl, pH 8.0, 10% *w*/*v* PEG 8000). The crystals were incubated for 5 min before being transferred to the cryoprotectant solution (100 mM Tris-HCl, pH 8.0, 10% *w*/*v* PEG 8000, 20% glycerol) for 10 min. The crystals were then incubated in the same solution containing an additional 1 mM of inhibitor **1** (SGT449) or **2** (SGT335) for 30 min and frozen in liquid nitrogen by rapid immersion. For Eis-

3 (SGT416) crystals, we used the above protocol, with the exception of using 100 mM Tris-HCl, pH 8.5 and 12.5% *w*/*v* PEG 8000 in the respective solutions.

The X-ray diffraction data was collected at the synchrotron beamline 22-ID of the Advanced Photon Source at the Argonne National Laboratory (Argonne, IL) at the wavelength of 1.00 Å at 100 K. The data were indexed, integrated and scaled with HKL2000.[8] The crystal structures were determined by molecular replacement using PHASER[9] and our original Eis structure (PDB ID: 3R1K)[1] as a search model. All the structures were in the R32 space group containing one Eis monomer per asymmetric unit. Readily interpretable strong electron density maps were observed for all complexes and used to build Eis bound inhibitors. The structures which were then built and refined iteratively using programs Coot[10] and REFMAC,[11] respectively. Crystallographic data and structure refinement statistics are summarized in Table S3. The Eis-**1** (SGT449), Eis-**2** (SGT335) and Eis-**3** (SGT416) structures were deposited in the Protein Data Bank (PDB) with accession numbers 6P3T, 6P3U, and 6P3V, respectively.

Table S3. X-ray diffraction data collection and structure refinement statistics for Eis-inhibitor complexes.

Eis-inhibitor complexes	Eis-**1** (SGT449)	Eis-**2** (SGT335)	Eis-**3** (SGT416)
PDB ID	6P3T	6P3U	6P3V
Data collection			
Space group	R32	R32	R32
Number of monomers per asymmetric unit	1	1	1
Unit cell dimensions			
a, b, c (Å)	175.6, 175.6, 122.7	175.4, 175.4, 122.9	174.9, 174.9, 121.5
α, β, γ (°)	90, 90, 120	90, 90, 120	90, 90, 120
Resolution (Å)	50.00-2.50 (2.54-2.50)[a]	50.0-2.55 (2.59-2.55)	50.0-2.50 (2.54-2.50)
R_{merge}	0.098 (0.669)	0.107 (0.612)	0.112 (0.654)
$CC_{1/2}$	0.998 (0.805)	0.992 (0.761)	0.991 (0.828)
$I/\sigma I$	17.9 (2.1)	16.1 (2.0)	16.7 (2.1)
Completeness (%)	99.6 (99.5)	99.7 (99.8)	97.9 (98.0)
Redundancy	5.0 (4.4)	5.7 (5.4)	5.1 (4.4)
Number of unique reflections	25046	24075	24278
Structure refinement statistics			
Resolution (Å)	35.00-2.50	35.00-2.55	34.57-2.50
R (%)	16.9	17.7	18.6
R_{free} (%)	20.5	20.6	22.0
R.m.s. deviations			
Bond lengths (Å)	0.005	0.006	0.006
Bond angles (°)	1.069	1.416	1.380
Ramachandran plot statistics[b]			
% of residues in favored region	99	98	98
% of residues in allowed region	1	2	2
% of residues in outlier region	0 (0 residues)	0	0

[a] Numbers in parentheses indicate the values in the highest-resolution shell.
[b] Indicates Rampage[12] statistics.

References

1. Chen, W.; Biswas, T.; Porter, V. R.; Tsodikov, O. V.; Garneau-Tsodikova, S., Unusual regioversatility of acetyltransferase Eis, a cause of drug resistance in XDR-TB. *Proc. Natl. Acad. Sci., U. S. A.* **2011,** *108* (24), 9804-9808. DOI: 10.1073/pnas.1105379108.
2. Ngo, H. X.; Green, K. D.; Gajadeera, C. S.; Willby, M. J.; Holbrook, S. Y. L.; Hou, C.; Garzan, A.; Mayhoub, A. S.; Posey, J. E.; Tsodikov, O. V.; Garneau-Tsodikova, S., Potent 1,2,4-triazino[5,6 b]indole-3-thioether inhibitors of the kanamycin resistance enzyme Eis from *Mycobacterium tuberculosis*. *ACS Infect. Dis.* **2018,** *4* (6), 1030-1040. DOI: 10.1021/acsinfecdis.8b00074.
3. Garzan, A.; Willby, M. J.; Ngo, H. X.; Gajadeera, C. S.; Green, K. D.; Holbrook, S. Y.; Hou, C.; Posey, J. E.; Tsodikov, O. V.; Garneau-Tsodikova, S., Combating enhanced intracellular survival Eis-mediated kanamycin resistance of *Mycobacterium tuberculosis* by novel pyrrolo[1,5-a]pyrazine-based Eis inhibitors. *ACS Infect. Dis.* **2017,** *3* (4), 302-309. DOI: 10.1021/acsinfecdis.6b00193.
4. Houghton, J. L.; Biswas, T.; Chen, W.; Tsodikov, O. V.; Garneau-Tsodikova, S., Chemical and structural insights into the regioversatility of the aminoglycoside acetyltransferase Eis. *ChemBioChem* **2013,** *14* (16), 2127-2135. DOI: 10.1002/cbic.201300359.
5. Willby, M. J.; Green, K. D.; Gajadeera, C. S.; Hou, C.; Tsodikov, O. V.; Posey, J. E.; Garneau-Tsodikova, S., Potent inhibitors of acetyltransferase Eis overcome kanamycin resistance in *Mycobacterium tuberculosis*. *ACS Chem. Biol.* **2016,** *11* (6), 1639-1646. DOI: 10.1021/acschembio.6b00110.
6. Garzan, A.; Willby, M. J.; Green, K. D.; Gajadeera, C. S.; Hou, C.; Tsodikov, O. V.; Posey, J. E.; Garneau-Tsodikova, S., Sulfonamide-based inhibitors of aminoglycoside acetyltransferase Eis abolish resistance to kanamycin in *Mycobacterium tuberculosis*. *J. Med. Chem.* **2016,** *59* (23), 10619-10628. DOI: 10.1021/acs.jmedchem.6b01161.
7. Tsodikov, O. V.; Green, K. D.; Garneau-Tsodikova, S., A random sequential mechanism of aminoglycoside acetylation by *Mycobacterium tuberculosis* Eis protein. *PLoS One* **2014,** *9* (4), e92370. DOI: 10.1371/journal.pone.0092370.
8. Otwinowski, Z.; Minor, W., Processing of X-ray diffraction data collected in oscillation mode. *Methods Enzymol.* **1997,** *276*, 307-326. DOI: 10.1016/S0076-6879(97)76066-X.

9. McCoy, A. J.; Grosse-Kunstleve, R. W.; Adams, P. D.; Winn, M. D.; Storoni, L. C.; Read, R. J., Phaser crystallographic software. *J. Appl. Cryst.* **2007,** *40* (Pt 4), 658-674. DOI: 10.1107/S0021889807021206.
10. Emsley, P.; Cowtan, K., Coot: model-building tools for molecular graphics. *Acta Cryst. D* **2004,** *60* (Pt 12 Pt 1), 2126-2132. DOI: 10.1107/S0907444904019158.
11. Murshudov, G. N.; Vagin, A. A.; Dodson, E. J., Refinement of macromolecular structures by the maximum-likelihood method. *Acta Cryst. D* **1997,** *53* (Pt 3), 240-255. DOI: 10.1107/S0907444996012255.
12. Lovell, S. C.; Davis, I. W.; Arendall, W. B., 3rd; de Bakker, P. I.; Word, J. M.; Prisant, M. G.; Richardson, J. S.; Richardson, D. C., Structure validation by Calpha geometry: phi,psi and Cbeta deviation. *Proteins* **2003,** *50* (3), 437-450. DOI: 10.1002/prot.10286.